This article was downloaded by: [Renmin University of China]
On: 13 October 2013, At: 10:46
Publisher: Taylor & Francis
Informa Ltd Registered in England and Wales Registered Number: 1072954 Registered office: Mortimer House, 37-41 Mortimer Street, London W1T 3JH, UK

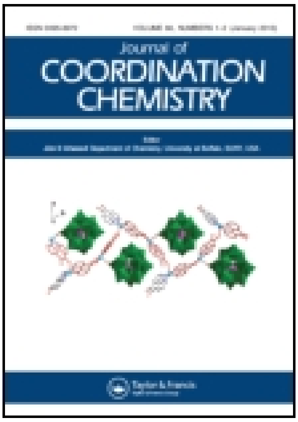

Journal of Coordination Chemistry
Publication details, including instructions for authors and subscription information:
http://www.tandfonline.com/loi/gcoo20

Syntheses and structural characterizations of three transition metal coordination complexes based on flexible 2,4-dichlorophenoxyacetate (2,4-DCP)

De-Yun Ma [a] , Hai-Fu Guo [a] , Kuan Lu [a] , Yong Pan [a] & Liang Qin [a]
[a] School of Chemistry and Chemical Engineering, Zhaoqing University , Zhaoqing 526061 , P.R. China

Published online: 05 Apr 2012.

To cite this article: De-Yun Ma , Hai-Fu Guo , Kuan Lu , Yong Pan & Liang Qin (2012) Syntheses and structural characterizations of three transition metal coordination complexes based on flexible 2,4-dichlorophenoxyacetate (2,4-DCP), Journal of Coordination Chemistry, 65:9, 1610-1620, DOI: 10.1080/00958972.2012.677040

To link to this article: http://dx.doi.org/10.1080/00958972.2012.677040

PLEASE SCROLL DOWN FOR ARTICLE

Taylor & Francis makes every effort to ensure the accuracy of all the information (the “Content”) contained in the publications on our platform. However, Taylor & Francis, our agents, and our licensors make no representations or warranties whatsoever as to the accuracy, completeness, or suitability for any purpose of the Content. Any opinions and views expressed in this publication are the opinions and views of the authors, and are not the views of or endorsed by Taylor & Francis. The accuracy of the Content should not be relied upon and should be independently verified with primary sources of information. Taylor and Francis shall not be liable for any losses, actions, claims, proceedings, demands, costs, expenses, damages, and other liabilities whatsoever or howsoever caused arising directly or indirectly in connection with, in relation to or arising out of the use of the Content.

This article may be used for research, teaching, and private study purposes. Any substantial or systematic reproduction, redistribution, reselling, loan, sub-licensing, systematic supply, or distribution in any form to anyone is expressly forbidden. Terms &

Journal of Coordination Chemistry
Vol. 65, No. 9, 10 May 2012, 1610–1620

Taylor & Francis
Taylor & Francis Group

Syntheses and structural characterizations of three transition metal coordination complexes based on flexible 2,4-dichlorophenoxyacetate (2,4-DCP)

DE-YUN MA*, HAI-FU GUO, KUAN LU, YONG PAN and LIANG QIN*

School of Chemistry and Chemical Engineering, Zhaoqing University,
Zhaoqing 526061, P.R. China

(*Received 6 December 2011; in final form 28 February 2012*)

Three transition metal coordination complexes, $\{[Co(2,4\text{-DCP})_2(\mu_2\text{-}H_2O)(H_2O)_2]\cdot(H_2O)_2\}_n$ (**1**), $[Zn(2,4\text{-DCP})(IN)]_n$ (**2**), and $[Mn_2(2,4\text{-DCP})_3(DMPY)_2(\mu_2\text{-}H_2O)(H_2O)]\cdot(2,4\text{-DCP})\cdot 0.2(H_2O)$ (**3**) (2,4-DCP = 2,4-dichlorophenoxyacetate, IN = isonicotinate, DMPY = 5,5′-dimethyl-2,2′-bipyridine), have been prepared under hydrothermal conditions and characterized by elemental analysis, IR spectroscopy, thermogravimetric analysis, and single-crystal X-ray diffraction. Complex **1** displays a 1-D chain through cobalt and bridging water molecules with Co···Co distance of 4.028(2) Å. Complex **2** shows a 2-D (4,4) net, which is extended into a 3-D supramolecular framework by weak hydrogen-bonding interactions. Complex **3** consists of discrete dinuclear cations, 2,4-DCP counter ions and free water molecules, which are assembled into a packing structure through $\pi\cdots\pi$ stacking of inversion-related DMPY ligands and hydrogen bonds. Magnetic susceptibility measurements show weak antiferromagnetic interactions in **1**. The photoluminescence and lifetime of **2** in the solid state have also been studied.

Keywords: Hydrothermal synthesis; Crystal structure; 2,4-Dichlorophenoxyacetate; Magnetic properties; Luminescent properties

1. Introduction

Coordination complexes have intriguing architectures, topologies, and applications in areas such as catalysis, separation, sorption, luminescence, magnetism, and biological chemistry [1–6]. Construction of coordination polymers depends on metal ions, organic ligands, solvent system, synthetic methods, pH, reaction temperature [7, 8], especially selection and utilization of building blocks. Fascinating coordination polymers have been constructed by carboxylate and/or N-containing ligands [9, 10] because of their ability to possess unusual structures and their sensitivity to molecular environments. 2,4-Dichlorophenoxyacetate (2,4-DCP) has various coordination modes. For example, Shi *et al*. [11] obtained three lanthanide complexes involving 1,10-phenanthroline and phenoxyacetic acid or 2,4-dichlorophenoxyacetic acid, two binuclear and another a 1-D polymeric structure. Dendrinou-Samara *et al*. [12] successfully synthesized two 1-D

---

*Corresponding authors. Email: mady@zqu.edu.cn; liangq@zqu.edu.cn

Journal of Coordination Chemistry
ISSN 0095-8972 print/ISSN 1029-0389 online © 2012 Taylor & Francis
http://dx.doi.org/10.1080/00958972.2012.677040

coordination polymers, which both exhibit antimicrobial action at concentrations under 1600 μg mL^{-1}.

As part of an on-going study related to transition metal carboxylates, we report preparation and structural characterization of three new coordination complexes $\{[Co(2,4\text{-}DCP)_2(\mu_2\text{-}H_2O)(H_2O)_2]\cdot(H_2O)_2\}_n$ (**1**), $[Zn(2,4\text{-}DCP)(IN)]_n$ (**2**), and $[Mn_2(2,4\text{-}DCP)_3(DMPY)_2(\mu_2\text{-}H_2O)(H_2O)]\cdot(2,4\text{-}DCP)\cdot 0.2(H_2O)$ (**3**). Complex **1** is a 1-D polymer with bridging water. Complex **2** shows a 2-D (4,4) net, which is extended into a 3-D supramolecular framework by weak hydrogen bonds. Complex **3** is dinuclear, assembled into a supramolecular network through $\pi\cdots\pi$ stacking of inversion-related 5,5′-dimethyl-2,2′-bipyridine (DMPY) ligands and hydrogen-bonding interactions. The structures of **1**–**3**, magnetic properties of **1,** and photoluminescence of **2** are reported in this article.

2. Experimental

2.1. *Materials and physical measurements*

All chemicals were commercially available and used as received. Elemental analyses for C, H, and N were carried out using a Vario EL III Elemental Analyzer. Infrared (IR) spectra were recorded (4000–400 cm^{-1}) as KBr discs on a Shimadzu IR-440 spectrometer for **1** and a Bruker 1600 FT-IR spectrometer for **2** and **3**. Luminescence spectra and lifetimes for crystal samples were recorded at room temperature on an Edinburgh FLS920 phosphorimeter. Thermogravimetric analysis (TGA) were performed on a simultaneous SDT thermal analyzer (STA449C, Netzsch) under a flow of N_2 at a heating rate of 10°C min^{-1} between ambient temperature and 800°C. Magnetic properties were studied using a Quantum Design SQUID magnetometer on the MPMS-7 system.

2.2. *Hydrothermal synthesis*

2.2.1. $\{[Co(2,4\text{-}DCP)_2(\mu_2\text{-}H_2O)(H_2O)_2]\cdot(H_2O)_2\}_n$ (1). Complex **1** was prepared by addition of stoichiometric amounts of $Co(NO_3)_2\cdot 6H_2O$ (0.145 g, 0.5 mmol) to a hot aqueous solution (10 mL) of 2,4-dichlorophenoxyacetic acid (0.110 g, 0.5 mmol). The pH was then adjusted to 7–8 with NaOH (0.01 g, 0.25 mmol). The resulting solution was filtered and pink single crystals were obtained at room temperature over a period of several days on slow evaporation of solvent (yield 57% based on 2,4-DCP). Anal. Calcd for $C_{16}H_{20}Cl_4CoO_{11}$ (**1**): C, 32.59; H, 3.40. Found: C, 32.65; H, 3.36. IR brands (KBr pellets, cm^{-1}): 3571(s), 3422(s), 1590(s), 1479(s), 1416(m), 1338(w), 1294(m), 1264(w), 1232(m), 1106(w), 1074(m), 869(w), 841(w), 808(m), 768(w), 721(m), 649(w).

2.2.2. $[Zn(2,4\text{-}DCP)(IN)]_n$ (2). A mixture of $Zn(NO_3)_2\cdot 6H_2O$ (0.150 g, 0.5 mmol), isonicotinic acid (0.06 g, 0.5 mmol), 2,4-dichlorophenoxyacetic acid (0.11 g, 0.5 mmol), NaOH (0.08 g, 0.2 mmol), and water (10 mL) was heated at 160°C for 72 h; colorless crystals were obtained upon cooling to room temperature at 5°C h^{-1} (yield: 51% based on 2,4-DCP). Anal. Calcd for $C_{14}H_9Cl_2NO_5Zn$ (**2**): C, 41.23; H, 2.21; N, 3.44.

Found (%): C, 41.25; H, 2.25; N, 3.40. IR (KBr pellet, cm^{-1}): 3435(s), 2022(s), 1658(s), 1578(m), 1526(w), 1477(m), 1406(s), 1285(m), 1225(m), 1092(w), 1063(m), 942(w), 882(m), 820(m), 770(m), 690(s).

2.2.3. $[Mn_2(2,4\text{-}DCP)_3(DMPY)_2(\mu_2\text{-}H_2O)(H_2O)]\cdot(2,4\text{-}DCP)\cdot0.2(H_2O)$ (3). A mixture of $MnCl_2\cdot2H_2O$ (0.09 g, 0.5 mmol), 5,5′-dimethyl-2,2′-bipyridine (0.092 g, 0.5 mmol), 2,4-dichlorophenoxyacetic acid (0.11 g, 0.5 mmol), NaOH (0.08 g, 0.2 mmol), and water (10 mL) was heated at 150°C for 72 h; colorless crystals were obtained upon cooling to room temperature at 5°C h^{-1} (yield: 55% based on 2,4-DCP). Anal. Calcd for $C_{56}H_{48.4}Cl_8Mn_2N_4O_{14.2}$ (**3**): C, 48.19; H, 3.44; N, 4.02. Found: C, 48.25; H, 3.50; N, 3.97. IR (KBr pellet, cm^{-1}): 3481(s), 1643(s), 1481(s), 1425(m), 1288(m), 1234(m), 1070(w), 1042(w), 817(w), 717(w), 646(w), 607(w).

2.3. *X-ray crystallography*

X-ray diffraction for **1**, **2**, and **3** were performed on a Bruker Apex II CCD diffractometer operating at 50 kV and 30 mA using Mo-Kα radiation ($\lambda = 0.71073$ Å) at room temperature. Data collection and reduction were performed using APEX II software [13]. Multi-scan absorption corrections were applied for all data sets using SADABS [13]. The structures were solved by direct methods and refined by least-squares on F^2 using the SHELXTL program package [13]. All non-hydrogen atoms were refined with anisotropic displacement parameters. Uncoordinated water of **3** is disordered with an occupancy factor of 0.20 (2). Hydrogen atoms attached to carbon were placed in geometrically idealized positions and refined using a riding model. Water hydrogen atoms were tentatively located in difference Fourier maps and refined with distance restraints of O–H = 0.84 Å and H $\cdots$ H = 1.39 Å, with an assigned standard deviation of 0.01 Å, and with $U_{iso}(H) = 1.5U_{eq}(O)$. Crystallographic data for **1**, **2**, and **3** are listed in table 1. Selected bond lengths and angles, and H-bonding parameters for the compounds are given in tables S1 and S2.

3. Results and discussion

3.1. $\{[Co(2,4\text{-}DCP)_2(\mu_2\text{-}H_2O)(H_2O)_2]\cdot(H_2O)_2\}_n$ (1)

Single-crystal X-ray diffraction analysis reveals that **1** shows a 1-D zigzag chain directed by μ_2-H_2O and 2,4-DCP linkers. A thermal ellipsoid plot of **1** is shown in figure 1(a). In the asymmetric unit of **1**, there are one Co(II), two 2,4-DCP anions, four coordinated water molecules, and two lattice water molecules. Co(II) is surrounded by two oxygen atoms of two monodentate 2,4-DCP ligands (scheme 1a) and four water molecules in octahedral geometry. The Co–O bond lengths and O–Co–O angles, all of which are within the range of those observed for analogous Co complexes [14–16], range from 2.040(4) Å to 2.200(3) Å and 87.26(15)° to 179.7(2)°. Neighboring $[Co(2,4\text{-}DCP)_2(H_2O)_2]$ units are connected into a 1-D zigzag chain (figure 1b). These chains are extended into 2-D sheets perpendicular to the *b*-axis *via* inter/intramolecular O–H $\cdots$ O hydrogen bonds (figure 2). The structure of **1** is similar to that of analogous

Table 1. Crystal data and structure refinement details of **1**, **2**, and **3**.

Compounds	**1**	**2**	**3**
Empirical formula	$C_{16}H_{20}Cl_4CoO_{11}$	$C_{14}H_9Cl_2NO_5Zn$	$C_{56}H_{48.4}Cl_8Mn_2N_4O_{14.2}$
Formula weight	589.05	407.49	1398.07
Temperature (K)	296(2)	296(2)	296(2)
Crystal system	Orthorhombic	Monoclinic	Triclinic
Space group	$Pna2_1$	$P2_1/c$	$P-1$
Unit cell dimensions (Å, °)			
a	8.0559(4)	8.0506(6)	8.030(2)
b	8.0553(4)	14.4153(10)	16.103(4)
c	37.139(2)	14.9766(8)	24.851(7)
α			102.951(6)
β		119.514(3)	91.440(5)
γ			99.339(5)
Volume (Å^3), Z	2410.0(2), 4	1512.52(17), 4	3083.7(14), 2
Calculated density (g cm^{-3})	1.623	1.789	1.506
$F(000)$	1196	816	1424
Crystal size (mm^3)	$0.35 \times 0.30 \times 0.25$	$0.33 \times 0.30 \times 0.21$	$0.32 \times 0.25 \times 0.18$
θ range for data collection (°)	1.10–25.19	2.11–25.20	1.39–25.20
Reflections collected	19,387	11,305	43,149
Independent reflections	4263	2709	11031
Goodness-of-fit on F^2	1.066	1.115	1.032
Final R indices [$I > 2\sigma(I)$]	$R_1 = 0.0431$, $wR_2 = 0.1240$	$R_1 = 0.0348$, $wR_2 = 0.1139$	$R_1 = 0.0476$, $wR_2 = 0.1378$
R indices (all data)	$R_1 = 0.0506$, $wR_2 = 0.1153$	$R_1 = 0.0436$, $wR_2 = 0.1049$	$R_1 = 0.0819$, $wR_2 = 0.1883$

$R_1 = \sum(||F_o| - |F_c||)/\sum|F_o|$. $wR_2 = [\sum w(F_o^2 - F_c^2)^2/\sum w(F_o)^2]^{1/2}$.

cobalt complexes of 2,6-dimethoxybenzoic acid (dmba) [14], 3-hydroxy-4-methoxybenzoic acid (hmba) [15], and other analogs such as the Co^{II}, Fe^{II}, and Ni^{II} hippurates [17, 18]. In the present complex the Co–H$_2$O–Co bridge is bent with an angle of 133.00° and the Co–Co distance is 4.028(2) Å. The corresponding values for dmba and hmba complexes are 132.3°, 3.96(7) Å and 128.06°, 4.082(3) Å, respectively. The Co–O$_{(\text{bridge})}$ (2.192–2.200 Å) distance of **1** is between hmba complex (2.270 Å) and dmba complex (2.070 Å).

3.2. *[Zn(2,4-DCP)(IN)]$_n$ (2)*

Complex **2** crystallizes in the monoclinic $P2_1/c$ space group and forms a 2-D square network. The fundamental unit of **2** contains one Zn^{2+}, one 2,4-DCP anion, and one IN anion. Each Zn^{2+} ion is five coordinate in a distorted square-pyramidal arrangement. The basal plane of each Zn^{2+} is surrounded by four oxygen atoms from two 2,4-DCP ligands and two IN ligands with Zn–O distances varying from 2.027(3) Å to 2.053(2) Å. The apical position is occupied by an IN nitrogen with Zn–N distance of 2.028(3) Å. As shown in the scheme (1b and c), 2,4-DCP ligand adopts a bridging mode to link two Zn(II) ions, while IN is μ_3 bridging linking three Zn(II) ions. Two neighboring five-coordinate Zn^{2+} ions are joined *via* four carboxylates of two 2,4-DCP ligands and two IN ligands, with the carboxylates bidentate bridging with Zn $\cdots$ Zn separation of 2.999(3) Å. The secondary building unit (SBU) is a paddle-wheel [Zn$_2$(COO)$_4$N$_2$] unit as shown in figure 3(a). Each paddle-wheel SBU is linked by IN ligands to form a 2-D

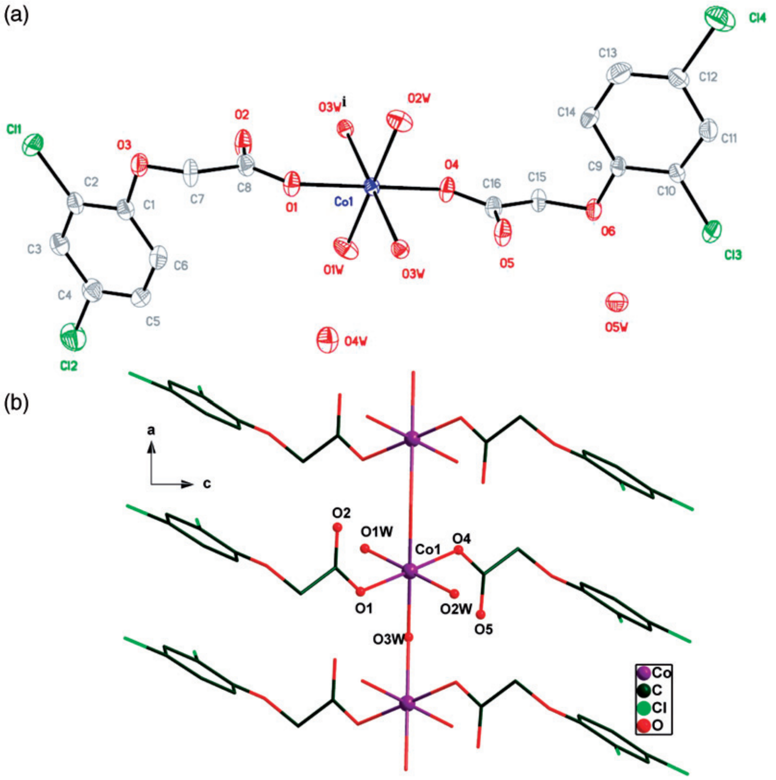

Figure 1. (a) Thermal ellipsoid plot of the asymmetric unit of **1** (30% probability ellipsoids) (symmetry code: $i = 0.5 + x,\ 1.5 - y,\ z$); (b) the infinite 1-D chain structure of **1**. All hydrogen atoms were omitted for clarity.

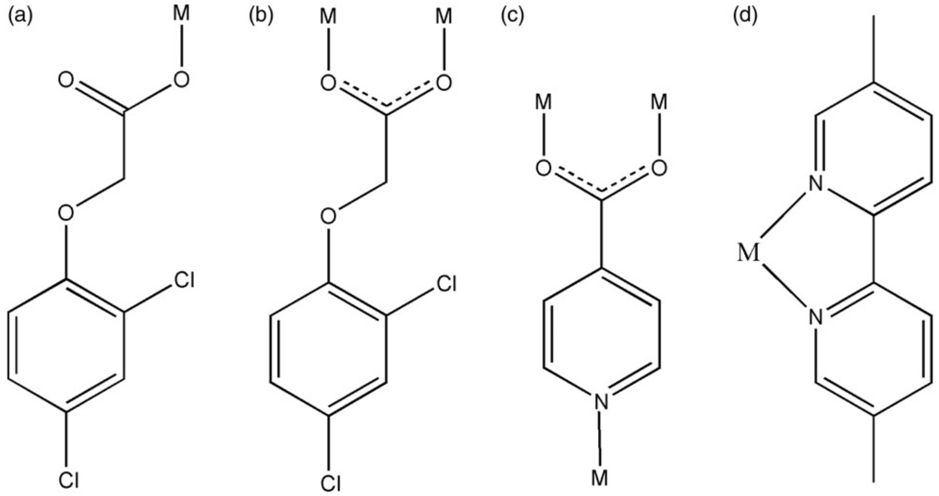

Scheme 1. The coordination mode of 2,4-DCP, IN, and DMPY ligands in the structures of **1**, **2**, and **3**.

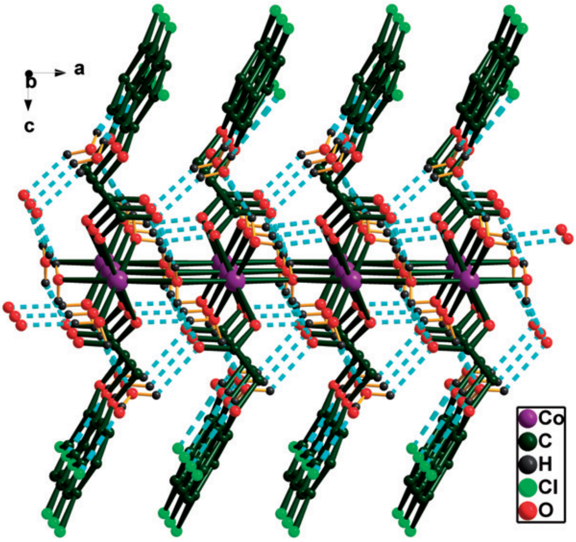

Figure 2. View of the 2-D sheet structure of **1** formed by hydrogen bonds, which are shown as sky blue dashed lines.

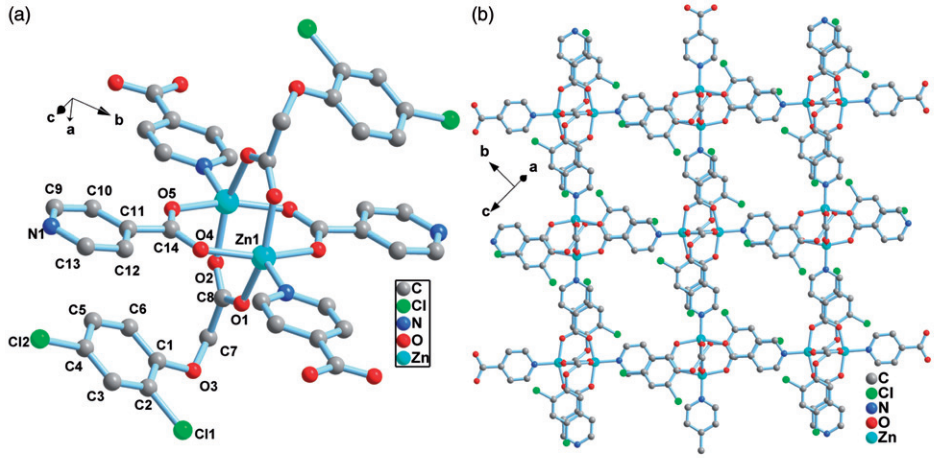

Figure 3. (a) Paddle-wheel [$Zn_2(COO)_4N_2$] unit of **2**; (b) 2-D layer of **2** viewed in the *bc*-plane of the cell. All hydrogen atoms were omitted for clarity.

layered network in the *bc*-plane of the cell in which the 2,4-DCP ligands point alternately up and down (figure 3b). This layered network is unusual, differing from those described by Lu and Runnels [19] and Liu *et al*. [20], which exhibit mutual-face-insertion layered open-framework and double-layer architecture, respectively. If both $(\mu_3\text{-IN})^-$ and paddle-wheel SBU are considered as quadruply connected nodes, then the overall 2-D super-structure of **2** is a (4,4) network. Neighboring layered networks are further connected into a 3-D supramolecular framework through

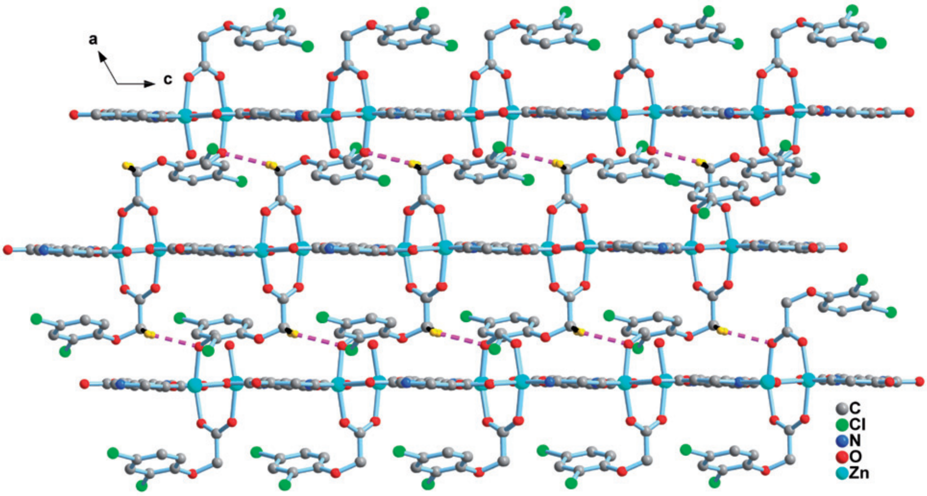

Figure 4. View of the 3-D supramolecular framework of **2** constructed by intra/intermolecular C–H · · · O hydrogen-bonding interactions (purple dashed lines).

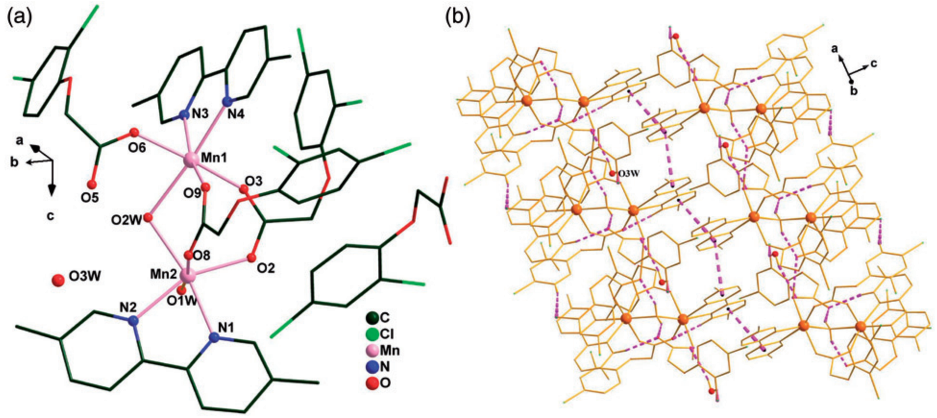

Figure 5. (a) View of the asymmetric unit of **3**; (b) 3-D packing structure of **3** with hydrogen-bonding interactions and $\pi \cdots \pi$ stacking interactions (purple dashed lines).

non-classical intermolecular C–H · · · O hydrogen-bonding interactions (figure 4). Intramolecular C–H · · · O hydrogen bonds are also observed.

3.3. *$[Mn_2(2,4\text{-}DCP)_3(DMPY)_2(\mu_2\text{-}H_2O)(H_2O)]\cdot(2,4\text{-}DCP)\cdot0.2(H_2O)$ (3)*

X-ray structure analysis shows that this complex is composed of a dinuclear $[Mn_2(2,4\text{-}DCP)_3(DMPY)_2(\mu_2\text{-}H_2O)(H_2O)]^+$ with two independent Mn^{2+} cations, separated by 3.700(2) Å, one 2,4-DCP^- and 0.20 uncoordinated water molecules, as illustrated in figure 5(a). Mn(1) is coordinated by two oxygen atoms of two bridging bidentate carboxylic groups of two 2,4-DCP ligands and one oxygen of monodentate carboxylic group of the other 2,4-DCP anions. The additional oxygen from water is involved in the bridging system. DMPY completes the distorted octahedral coordination around Mn(1). In contrast Mn(2) coordinates one water molecule. Together with three bridging oxygen atoms and two chelating nitrogen atoms an octahedral coordination is formed. The strains induced by bridging are responsible for the observed distortion of both octahedra. The carboxylate bridges are not symmetrical: in Mn(1)–O(3)–C(32)–O(2)–Mn(2), the Mn(1)–O(3) distance is 2.107(3) Å while the Mn(2)–O(2) bond length is 2.141(2) Å. In Mn(1)–O(9)–C(41)–O(8)–Mn(2), the Mn(1)–O(9) and Mn(2)–O(8) distances are also different: 2.166(4) Å and 2.154(5) Å, respectively. The Mn(1)–O(2W)–Mn(2) bridge shows a slight elongation compared to the Mn(2)–O(1W) distance (table S1). The structures are governed by inter/intramolecular O–H $\cdots$ O, O–H $\cdots$ Cl, C–H $\cdots$ O, C–H $\cdots$ Cl hydrogen bonds involving coordinated water, uncoordinated water, chloride, and carboxyl oxygen atoms of 2,4-DCP, and *via* $\pi \cdots \pi$ stacking interactions of neighboring pyridine rings of DMPY ligands, with the centroid to centroid distances of 3.622(7) and 3.753(5) Å (figure 5b).

3.4. *IR spectra*

FT-IR spectra of **1**–**3** are recorded as KBr pellets (figures S1–S3). Strong, broad bands at 3571, 3422 $\mathrm{cm^{-1}}$ in **1** may be assigned to ν(O–H) of water and 3435 $\mathrm{cm^{-1}}$ in **2** and 3481 $\mathrm{cm^{-1}}$ in **3** may be assigned to ν(O–H) of water. Features at 1590 and 1416 $\mathrm{cm^{-1}}$ for **1**, 1658, 1578, and 1406 $\mathrm{cm^{-1}}$ for **2**, and 1643 and 1425 $\mathrm{cm^{-1}}$ for **3** are associated with the asymmetric (C–O–C) and symmetric (C–O–C) stretches.

3.5. *TG analyses*

"Supplementary materials" (figures S4–S6) show the TG analyses performed on **1**, **2**, and **3** under nitrogen. Complex **1** shows two weight loss steps. The first corresponding to release of two free water molecules is observed from 30°C to 200°C (obsd 6.0%, Calcd 6.2%). The compound begins to decompose when the coordinated water molecules escape at 200°C. Complex **2** has thermal stability as no clean weight-loss step occurs below 210°C. The weight-loss step above 210°C corresponds to decomposition of the framework structure. Complex **3** shows a gradual weight loss of 15.6% (25–200°C), corresponding to the escape of one free 2,4-DCP anion and 0.2 free water molecules (Calcd 15.9%). Then a sharp weight loss occurs above 200°C due to decomposition of the cation.

3.6. *Magnetic susceptibility of 1*

The magnetic properties of **1** in the form of $\chi_M T$ *versus* T and χ_M^{-1} *versus* T plots are shown in figure 6. The $\chi_M T$ value at 300 K is 2.31 $\mathrm{cm^3\,mol^{-1}\,K}$ for each cobalt, larger than expected for spin-only ($\chi_M T = 1.87\ \mathrm{cm^3\,mol^{-1}\,K}$, $S = 3/2$), indicating orbital contribution of the octahedral $\mathrm{Co^{II}}$ [21, 22]. $\chi_M T$ gradually decreases from room temperature and reaches a minimum of 0.65 $\mathrm{cm^3\,mol^{-1}\,K}$ at 8 K, then increases again to 1.51 $\mathrm{cm^3\,mol^{-1}\,K}$ at 4 K. The χ_M^{-1} *versus* T plot obeys Curie–Weiss law $\chi_M = C/(T - \theta)$

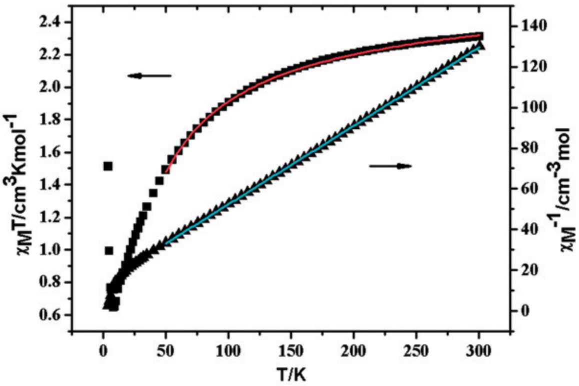

Figure 6. Plots of $\chi_M T$ and $1/\chi_M$ *vs.* T for **1**.

above 50 K with the value of the Curie constant, $C = 2.9\,\mathrm{cm^3\,K\,mol^{-1}}$, within the reported value of six-coordinate, high-spin Co(II) ($C = 2.8$–$3.4\,\mathrm{cm^3\,K\,mol^{-1}}$) [21, 22]; the negative sign of $\theta = -36.02$ K originates from a significant orbital contribution and/or antiferromagnetic coupling between Co^{2+}.

In **1**, the adjacent Co(II) was bridged by coordination water to form a 1-D Co–O–Co chain with Co–Co distance of 4.028 Å. To investigate the magnetic behavior of **1**, we can fit the experimental data to 49 K using Line model ($S = 3/2$) with the simple equation (figure S7), and we get values for the intraline exchange parameter J and the Landé g-factor from this formula ($-7.01\,\mathrm{cm^{-1}}$ and 2.30, respectively). The J value is close to the previously reported value of $-7.0\,\mathrm{cm^{-1}}$ [23]. A molecular field correction should also be taken into account in the mean-field approximation with the parameter $zJ' = -1.31\,\mathrm{cm^{-1}}$ as the magnetic interaction between chains. As expected, water oxygen can also be used as the path of magnetic exchange.

3.7. *Luminescent properties of 2*

Solid-state excitation and emission luminescence spectra of **2** at room temperature are shown in figure 6. Complex **2** exhibits indigotin photoluminescence with an emission maximum at *ca* 420 nm upon excitation at 322 nm (figure 7). Usually energy transitions of d^{10} complexes can be assigned as metal-to-ligand charge-transfer, intraligand emission, and ligand-to-metal charge-transfer. As previously reported [24], the photoluminescence mechanism of title compound is tentatively attributed to ligation of the ligand to the metal center. Moreover, as shown in figure 8, the luminescent lifetime of solid **1** using an Edinburgh FLS920 phosphorimeter with a 450 W xenon lamp as excitation source is 175.1 ns.

4. Conclusion

Based on hydrothermal method, three new transition metal coordination complexes based on flexible 2,4-DCP have been synthesized and structurally characterized.

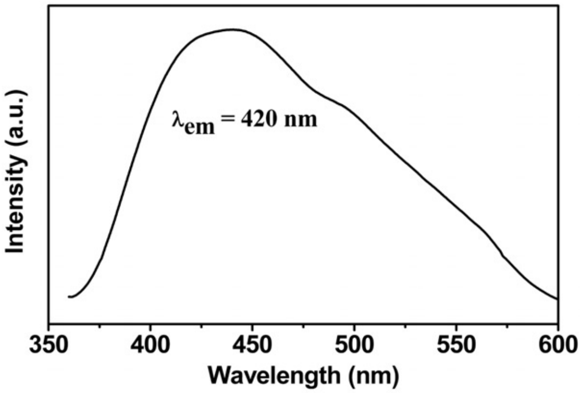

Figure 7. Solid-state emission spectrum of **2** at room temperature (excited at 322 nm).

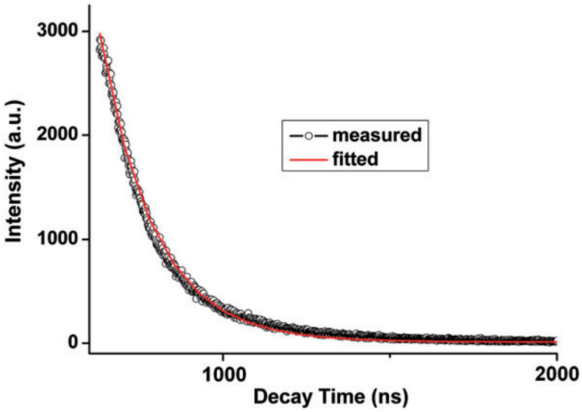

Figure 8. Luminescent lifetime of **2**.

Complex **1** displays a 1-D chain through cobalt and bridging water molecules. Complex **2** shows a layered network. Complex **3** consists of discrete dinuclear cations, 2,4-DCP counter ions, and uncoordinated water. Magnetic studies indicate that the interactions between Co(II) ions of **1** is antiferromagnetic. Complex **2** displays intense blue photoluminescence with lifetime of 175.1 ns in the solid state at room temperature and could be a candidate as blue light-emitting luminescent materials. Further work on other coordination polymers with intriguing architectures and properties based on this ligand is ongoing in our laboratory.

Supplementary material

Crystallographic data for the structural analysis have been deposited with the Cambridge Crystallographic Data Centre; CCDC references numbers are 710505, 854935, and 854936 for **1**, **2**, and **3**. Copies of this information may be obtained free of charge on application to CCDC, 12 Union Road, Cambridge CB2 1EZ, UK (Fax: +44-1223-336-033; E-mail: deposit@ccdc.cam.ac.uk or www: http://www.ccdc.cam.ac.uk). The additional figures can be obtained from the web free of cost.

Acknowledgments

We thank the Zhaoqing University with doctor start-up fund for the financial support.

References

[1] Y.G. Huang, F.L. Jiang, M.C. Hong. *Coord. Chem. Rev.*, **253**, 2814 (2009).
[2] D. Ma, W. Wang, Y. Li, J. Li, C. Diaguebonne, G. Calvez, O. Guillou. *CrystEngComm*, **12**, 4372 (2010).
[3] O.M. Yaghi, M. O'Keeffe, N.W. Ockwig, H.K. Chae, M. Eddaoudi, J. Kim. *Nature*, **423**, 705 (2003).
[4] D. Ma, Y. Li, Z. Li. *Chem. Commun.*, **47**, 7377 (2011).
[5] J.R. Long, O.M. Yaghi. *Chem. Soc. Rev.*, **38**, 1213 (2009).
[6] H.Y. Wu, S.T. Yue, N. Wang, Y.L. Liu. *J. Coord. Chem.*, **63**, 785 (2010).
[7] A.S. Rao, A. Pal, R. Ghosh, S.K. Das. *Inorg. Chem.*, **48**, 1802 (2009).
[8] L. Liu, S.P. Huang, G.D. Yang, H. Zhang, X.L. Wang, Z.Y. Fu, J.G. Dai. *Cryst. Growth Des.*, **10**, 930 (2010).
[9] (a) J.Q. Liu. *J. Coord. Chem.*, **64**, 1503 (2011); (b) J.Q. Liu. *J. Coord. Chem.*, **64**, 1807 (2011).
[10] J.Y. Lee, D.H. Olson, L. Pan, T.J. Emge, J. Li. *Adv. Funct. Mater.*, **17**, 1255 (2007).
[11] S.M. Shi, Z.F. Chen, Y.C. Liu, L. Mao, H. Liang, Z.Y. Zhou. *J. Coord. Chem.*, **61**, 2725 (2008).
[12] C. Dendrinou-Samara, D. Drosou, L. Iordanidis, A. Terzis, D.P. Kessissoglou. *J. Inorg. Biochem.*, **92**, 156 (2002).
[13] (a) Bruker. *APEX II Software (Version 6.3.1)*, Bruker AXS Inc., Madison, Wisconsin, USA (2004); (b) G.M. Sheldrick. *Acta Cryst.*, **A64**, 112 (2008).
[14] L. Strinna Erre, G. Micera, F. Cariati, G. Ciani, A. Sironi, H. Kozlowski, J. Baranowski. *J. Chem. Soc., Dalton Trans.*, 363 (1988).
[15] T. Glowiak, H. Kozlowski, L. Strinna Erre, B. Gulinati, G. Micera, A. Pozzi, S. Bruni. *J. Coord. Chem.*, **25**, 75 (1992).
[16] (a) C.H. Ng, S.G. Teoh, N. Moris, S.Y. Yap. *J. Coord. Chem.*, **57**, 1037 (2004); (b) M.R. Barton, Y. Zhang, J.D. Atwood. *J. Coord. Chem.*, **55**, 969 (2002).
[17] M.M. Morelock, M.L. Good, L.M. Trefonas, D. Karraker, L. Maleki, H.R. Eichelberger, R. Majeste, J. Dodge. *J. Am. Chem. Soc.*, **101**, 4858 (1979).
[18] M.M. Morelock, M.L. Good, L.M. Trefonas, R. Majeste, D.G. Karraker. *Inorg. Chem.*, **21**, 3044 (1982).
[19] J.Y. Lu, K.A. Runnels. *Inorg. Chem. Commun.*, **4**, 678 (2001).
[20] Z. Liu, P. Liu, Y. Chen, J. Wang, M. Huang. *New J. Chem.*, **29**, 474 (2005).
[21] F.E. Mabbs, D.J. Machin. *Magnetism and Transition Metal Complexes*, Chapman and Hall, London (1973).
[22] B.N. Figgis, M.A. Hitchman. *Ligand Field Theory and Its Applications*, Wiley-VCH, New York (2000).
[23] S.R. Marshall, C.D. Incarvito, J.L. Manson, A.L. Rheinhold, J.S. Miller. *Inorg. Chem.*, **39**, 1969 (2000).
[24] Z. Li, M. Li, X.P. Zhou, T. Wu, D. Li, S.W. Ng. *Cryst. Growth Des.*, **7**, 1992 (2007).